

Measurement of the CKM angles γ and $2\beta + \gamma$ at B factories

Jean-Pierre LEES

Laboratoire d'Annecy-le-Vieux de Physique des Particules (LAPP), IN2P3/CNRS et Université de Savoie,
9 Chemin de Bellevue, BP 110, F-74941 Annecy-le-Vieux CEDEX - FRANCE

On behalf of the BABAR and Belle collaborations, we report on the measurement of the angle γ and on the sum of angles $2\beta + \gamma$ of the Unitarity Triangle.

1. Introduction

The angle γ (or ϕ_3) of the unitarity triangle is related to the complex phase of the CKM matrix element V_{ub} through $V_{ub} = |V_{ub}|e^{-i\gamma}$. Various methods have been proposed to measure the angle γ . We report on two classes of measurements: time independent measurements in decays $B^\pm \rightarrow D^0/\bar{D}^0 K^\pm$ exploit the interference between the $b \rightarrow c\bar{u}s$ and the $b \rightarrow u\bar{c}s$ decay amplitudes and are sensitive to the angle γ ; time dependent asymmetries in decays $B^0 \rightarrow D^{(*)\pm}\pi^\mp$ or $B^0 \rightarrow D^0 K^0$ occur through the interference of the favored amplitude $B^0 \rightarrow \bar{D}^{(*)-}\pi^+$ ($B^0 \rightarrow \bar{D}^{(*)0}K^0$) and the suppressed amplitude $\bar{B}^0 \rightarrow \bar{D}^{(*)-}\pi^+$ ($\bar{B}^0 \rightarrow \bar{D}^{(*)0}K^0$) plus B^0/\bar{B}^0 mixing, and are sensitive to the sum of angles $2\beta + \gamma$.

2. Measurement of γ in $B^\pm \rightarrow D^0/\bar{D}^0 K^\pm$

The experimental techniques used to measure γ in charged B decays exploit the interference between $B^- \rightarrow D^{(*)0}K^{*-}$ and $B^- \rightarrow \bar{D}^{(*)0}K^{*-}$ (Fig. 1) that occurs when the $D^{(*)0}$ and the $\bar{D}^{(*)0}$ decay to common final states.

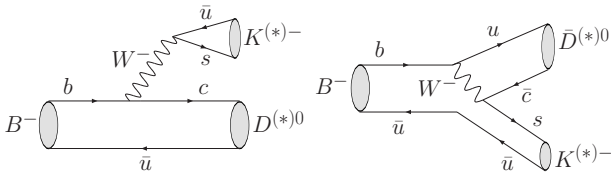


Figure 1: Feynman diagrams for $B^- \rightarrow D^{(*)0}K^{*-}$ and $\bar{D}^{(*)0}K^{*-}$. The latter is CKM and color suppressed with respect to the former. The CKM-suppression factor is $|V_{ub}V_{cs}^*/V_{cb}V_{us}^*| \approx 0.4$. The naive color-suppression factor is $\frac{1}{3}$.

Three different methods have been used so far:

- The GLW method [1]: the D^0 and the \bar{D}^0 decay to a CP eigenstate
- The ADS method [2]: the D^0 from the favored $b \rightarrow c$ amplitude is reconstructed in the doubly-Cabbibo suppressed final state $K^+\pi^-$, while the \bar{D}^0 from the $b \rightarrow u$ suppressed amplitude is reconstructed in the favored final state $K^+\pi^-$.

- The GGSZ (Dalitz) method [3]: the D^0 and the \bar{D}^0 are reconstructed in the same $K_S^0\pi^+\pi^-$ three body final state. This is based on the analysis of the $K_S^0\pi^+\pi^-$ Dalitz distribution and can to some extent be considered as a mixture of the two previous methods, depending on the position in the Dalitz plot.

In all three methods, the experimental observables depend on two additional parameters which need to be determined in order to extract useful constraints on the value of γ : the magnitude r_B of the ratio of the amplitudes for the processes $B^- \rightarrow \bar{D}^0 K^-$ and $B^- \rightarrow D^0 K^-$ (Fig. 1) and the relative strong phase δ_B between these two amplitudes. The amplitude ratio r_B and the phase δ_B are specific of each B decay mode reconstructed ($D^0 K$, $D^{*0} K$ and $D^0 K^*$).

2.1. The GLW method and results:

The results of the GLW analyses are usually expressed in terms of the ratios $R_{CP\pm}$ of charge-averaged partial rates and of the partial-rate charge asymmetries $A_{CP\pm}$,

$$R_{CP\pm} = \frac{\Gamma(B^- \rightarrow D_{CP\pm}^0 K^-) + \Gamma(B^+ \rightarrow D_{CP\pm}^0 K^+)}{[\Gamma(B^- \rightarrow D^0 K^-) + \Gamma(B^+ \rightarrow \bar{D}^0 K^+)]/2}, \quad (1)$$

$$A_{CP\pm} = \frac{\Gamma(B^- \rightarrow D_{CP\pm}^0 K^-) - \Gamma(B^+ \rightarrow D_{CP\pm}^0 K^+)}{\Gamma(B^- \rightarrow D_{CP\pm}^0 K^-) + \Gamma(B^+ \rightarrow D_{CP\pm}^0 K^+)}. \quad (2)$$

where $CP+$ refers to the CP-even final states $\pi^+\pi^-$ and K^+K^- and $CP-$ refers to the CP-odd final states $K_S^0\pi^0$, $K_S^0\phi$ and $K_S^0\omega$. $R_{CP\pm}$ and $A_{CP\pm}$ are related to the angle γ , the amplitude ratio r_B and the strong phase difference δ_B through the relations $R_{CP\pm} = 1 + r_B^2 \pm 2r_B \cos \delta_B \cos \gamma$ and $A_{CP\pm} = \pm 2r_B \sin \delta_B \sin \gamma / R_{CP\pm}$ [1], thus allowing a determination of the 3 unknowns (r_B , δ_B and γ) up to an 8 fold ambiguity in γ . The variation of R_{CP} and A_{CP} vs the strong phase δ_B for $r_B = 0.10$ is shown in Fig.2 for different values of γ . The asymmetries for $CP+$ and $CP-$ states have opposite signs, while the Bf ratios are approximately symmetric respective to 1. The GLW method is theoretically clean, with nearly no hadronic uncertainty. However, it is experimentally challenging, as the effective branching ratio for the decay modes reconstructed is of the or-

Table I Summary of *BABAR* and *Belle* measurements of the GLW observables R_{CP} and A_{CP} .

Mode	Experiment	$N(B\bar{B}) [10^6]$	A_{CP+}	A_{CP-}	R_{CP+}	R_{CP-}
$B \rightarrow D^0 K$	<i>BABAR</i> [4]	232	$+0.35 \pm 0.13 \pm 0.04$	$-0.06 \pm 0.13 \pm 0.04$	$0.90 \pm 0.12 \pm 0.04$	$0.86 \pm 0.10 \pm 0.05$
	<i>Belle</i> [5]	275	$+0.06 \pm 0.14 \pm 0.05$	$-0.12 \pm 0.14 \pm 0.05$	$1.13 \pm 0.16 \pm 0.08$	$1.17 \pm 0.14 \pm 0.14$
	HFAG Average [8]	-	$+0.22 \pm 0.10$	-0.09 ± 0.10	0.90 ± 0.10	0.94 ± 0.10
$B \rightarrow D^{*0} K$	<i>BABAR</i> [6]	123	$-0.10 \pm 0.23^{+0.03}_{-0.04}$	-	$1.06 \pm 0.26^{+0.10}_{-0.09}$	-
	<i>Belle</i> [5]	275	$-0.20 \pm 0.22 \pm 0.04$	$+0.13 \pm 0.30 \pm 0.08$	$1.41 \pm 0.25 \pm 0.06$	$1.15 \pm 0.31 \pm 0.12$
	HFAG Average [8]	-	-0.15 ± 0.16	$+0.13 \pm 0.31$	1.25 ± 0.19	1.15 ± 0.33
$B \rightarrow D^0 K^*$	<i>BABAR</i> [7]	232	$-0.08 \pm 0.19 \pm 0.08$	$-0.26 \pm 0.40 \pm 0.12$	$1.96 \pm 0.40 \pm 0.11$	$0.65 \pm 0.26 \pm 0.08$
	<i>Belle</i>	-	-	-	-	-
	HFAG Average [8]	-	-0.08 ± 0.21	-0.26 ± 0.42	1.96 ± 0.41	0.65 ± 0.27

der of 10^{-6} . Both *BABAR* and *Belle* reconstruct the CP-even and CP-odd modes listed above and have published recently final results using statistical samples larger than 200 million $B\bar{B}$ events. The corresponding numbers of reconstructed events are about 100 $CP+$ and 100 $CP-$ events in each experiment for the $B^- \rightarrow D^0 K^-$ modes, and even less for the modes $B^- \rightarrow D^{*0} K^-$ and $B^- \rightarrow D^0 K^{*-}$, which have a lower reconstruction efficiency. The ΔE distribution of $CP+$ and $CP-$ events in the *BABAR* $B^- \rightarrow D^0 K^-$ analysis is shown in Fig.3. The different *BABAR* and *Belle* $B^- \rightarrow D^{(*)0} K^{(*)-}$ analysis are described in detail in references [4, 5, 6, 7] and their results are summarized in Table I. Due to the limited statistics and to the smallness of the r_B parameter, the GLW method alone is not yet able to provide strong constraints on γ . For the $B^- \rightarrow D^0 K^-$ decay channel, 3σ significant differences between B^- and B^+ data seem to be within reach in the near future, when $\sim 1ab^{-1}$ of data will have been collected in each experiment.

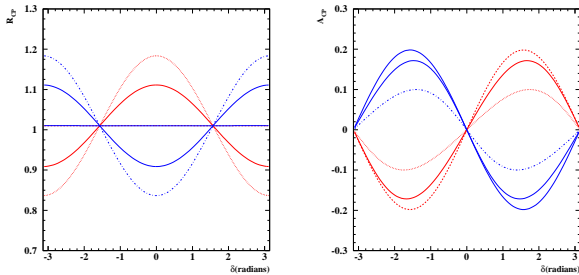


Figure 2: The variation of R_{CP} (left) and A_{CP} (right) vs the strong phase δ_B for $r_B = 0.10$ and $\gamma = 30^\circ, 60^\circ$ and 90° . Red is for $CP+$ modes and blue for $CP-$ modes.

2.2. ADS Results:

In the Atwood-Dunietz-Soni (ADS) method, instead of using CP eigenstate decays of the D^0 , the decays $D^0 \rightarrow K^+ \pi^-$ and $\bar{D}^0 \rightarrow K^+ \pi^-$ are used.

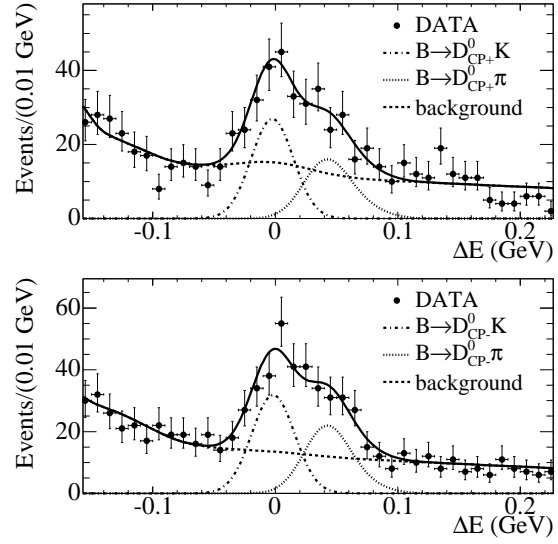


Figure 3: Distributions of ΔE for events enhanced in $B \rightarrow D^0 K$ signal at *BABAR*. Top: $B^- \rightarrow D^0_{CP+} K^-$; bottom: $B^- \rightarrow D^0_{CP-} K^-$. Solid curves represent projections of the maximum likelihood fit; dashed, dashed-dotted and dotted curves represent the $B \rightarrow D^0 K$, $B \rightarrow D^0 \pi$ and background contributions.

The overall effective branching ratio for the final state $B^- \rightarrow [K^+ \pi^-]_{D^0} K^-$ is expected to be small ($\sim 10^{-7}$), but the two interfering diagrams are of the same order of magnitude and large asymmetries are therefore expected. The favored decay mode $B^- \rightarrow [K^- \pi^+]_{D^0} K^-$ is used to normalize the measurement and cancel many experimental systematics. The main experimental observable are the ratio R_{ADS} of the suppressed to favored modes and the B^- / B^+ asymmetry:

$$\begin{aligned}
 R_{ADS} &= \frac{\mathcal{B}([K^+ \pi^-]_{D^0} K^-) + \mathcal{B}([K^- \pi^+]_{D^0} K^+)}{\mathcal{B}([K^- \pi^+]_{D^0} K^-) + \mathcal{B}([K^+ \pi^-]_{D^0} K^+)} \\
 &= r_D^2 + 2r_D r_B \cos \gamma \cos(\delta_B + \delta_D) + r_B^2 \quad (3) \\
 A_{ADS} &= \frac{\mathcal{B}([K^+ \pi^-]_{D^0} K^-) - \mathcal{B}([K^- \pi^+]_{D^0} K^+)}{\mathcal{B}([K^+ \pi^-]_{D^0} K^-) + \mathcal{B}([K^- \pi^+]_{D^0} K^+)}
 \end{aligned}$$

Table II Summary of BABAR and Belle ADS measurements.

Mode	Experiment	$N(B\bar{B}) [10^6]$	R_{ADS}	R_{ADS} 90% C.L.limit	r_B	r_B 90% C.L.limit
$B \rightarrow D^0 K$	BABAR[10]	232	$0.013^{+0.011}_{-0.009}$	< 0.029		$r_B < 0.23$
	Belle [12]	386	$0.000 \pm 0.008 \pm 0.001$	< 0.0139		$r_B < 0.18$
$B \rightarrow D_{(D^0\pi^0)}^* K$	BABAR[10]	232	$-0.002^{+0.010}_{-0.006}$	< 0.023		$r_B^{*2} < (0.16)^2$
$B \rightarrow D_{(D^0\gamma)}^* K$			$0.011^{+0.018}_{-0.013}$	< 0.045		
$B \rightarrow D^0 K^*$	BABAR[11]	232	$0.046 \pm 0.031 \pm 0.08$		$r_B = 0.28^{+0.006}_{-0.010}$	

$$= 2r_D r_B \sin \gamma \sin(\delta_B + \delta_D) / R_{ADS}, \quad (4)$$

where $r_B = |A(B^- \rightarrow \bar{D}^0 K^-) / A(B^- \rightarrow D^0 K^-)|$ and $r_D = |A(D^0 \rightarrow K^+ \pi^-) / A(D^0 \rightarrow K^- \pi^+)| = 0.060 \pm 0.003$ [9] are the suppressed to favored B and D amplitude ratios, and δ_B and δ_D are the strong phase differences between the two B and D decay amplitudes, respectively. As it can be seen from Eq. 3, R_{ADS} is highly sensitive to r_B^2 . Using a sample of $232 \times 10^6 B\bar{B}$ events, BABAR reconstructs 5^{+4}_{-3} events in the $B^- \rightarrow D^0 [K^+ \pi^-] K^-$ channel, $-0.2^{+1.3}_{-0.7}$ events in the $B^- \rightarrow D^{*0} [K^+ \pi^-] K^-$ channel ($D^{*0} \rightarrow D^0 \pi^0$), $1.2^{+2.1}_{-1.4}$ events in the $B^- \rightarrow D^{*0} [K^+ \pi^-] K^-$ channel ($D^{*0} \rightarrow D^0 \gamma$), and 4.2 ± 2.8 events in the $B^- \rightarrow D^0 [K^+ \pi^-] K^{*-}$ channel [10, 11]. From $386 \times 10^6 B\bar{B}$ events, Belle reconstructs $0.0^{+5.3}_{-5.0}$ events in the $B^- \rightarrow D^0 [K^+ \pi^-] K^-$ channel [12]. None of these results are statistically significant and for the $D^0 K$ and $D^{*0} K$ channels limits on R_{ADS} and r_B are extracted. The Belle result for $B^- \rightarrow D^0 K^-$ is illustrated in Fig.4. The least restrictive limit is obtained allowing $\pm 1\sigma$ variation on r_D and assuming maximal interference ($\gamma = 0^\circ$, $\delta_B + \delta_D = 180^\circ$ or $\gamma = 180^\circ$, $\delta_B + \delta_D = 0^\circ$) and is found to be $r_B < 0.18$ at 90% C.L.. For the BABAR $B^- \rightarrow D^0 [K^+ \pi^-] K^{*-}$ result, a frequentist approach has been used to combine the results from the GLW and ADS methods, resulting in $r_B = 0.28^{+0.06}_{-0.10}$ and excluding the interval $75^\circ < \gamma < 105^\circ$ at the two standard deviation level. A summary of the BABAR and Belle ADS results can be found in Table II, and more details on the analysis in Ref.[10, 11, 12]. Similar to the GLW analysis, more statistics are needed to constraint γ from the ADS method.

2.3. The $K_s^0 \pi^+ \pi^-$ Dalitz (GGSZ) Analysis:

A third method to constraint γ from $B^- \rightarrow D^0 K^-$ decays is to use three body final states common to D^0 and \bar{D}^0 , as suggested in Ref.[3]. Among the possible D^0 3-body decay modes the $K_s^0 \pi^+ \pi^-$ channel appears to have the largest sensitivity to γ , because of the best overall combination of branching ratio

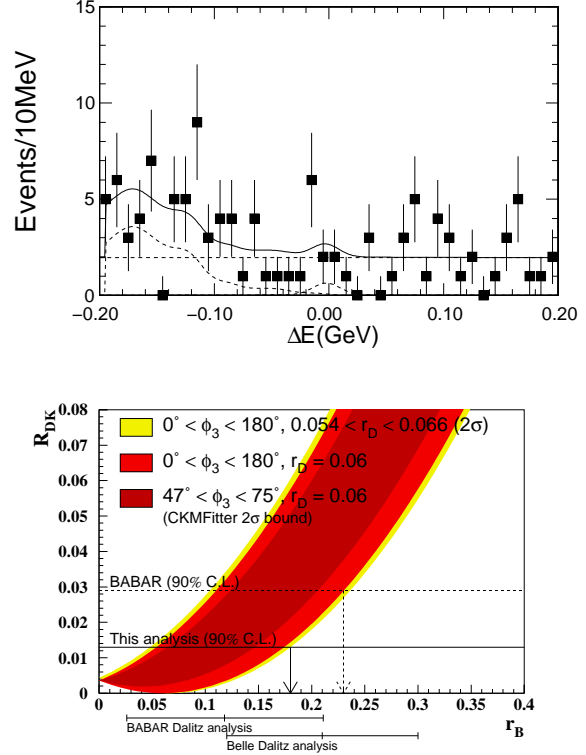


Figure 4: (Top) Belle ΔE fit results for $B^- \rightarrow D_{sup} K^-$. (Bottom) Belle constraint on r_B from R_{DK} .

magnitude, D^0 - \bar{D}^0 interference and background level. Defining the Dalitz plot amplitude of the decay $D^0 \rightarrow K_s^0 \pi^+ \pi^-$ as $A_D(m_-^2, m_+^2)$, where $m_-^2 = m^2(K_s^0 \pi^-)$ and $m_+^2 = m^2(K_s^0 \pi^+)$, the Dalitz plot density of the D^0 in $B^\pm \rightarrow D^0 K^\pm$ decays can be written as

$$d\sigma(m_\mp^2, m_\pm^2) \equiv |A_D(m_\mp^2, m_\pm^2)|^2 + r_B^2 |A_D(m_\pm^2, m_\mp^2)|^2 + 2r_B \text{Re}[A_D(m_\mp^2, m_\pm^2) A_D^*(m_\pm^2, m_\mp^2) e^{i(\delta_B \mp \gamma)}]. \quad (5)$$

Information on the weak phase γ , the strong phase difference δ_B and the ratio r_B of the two $B^\pm \rightarrow D^0 K^\pm$ decay amplitudes can be obtained from simultaneous fit of the Dalitz plot density of B^- and B^+ data if the Dalitz decay amplitude $A_D(m_\mp^2, m_\pm^2)$ is precisely

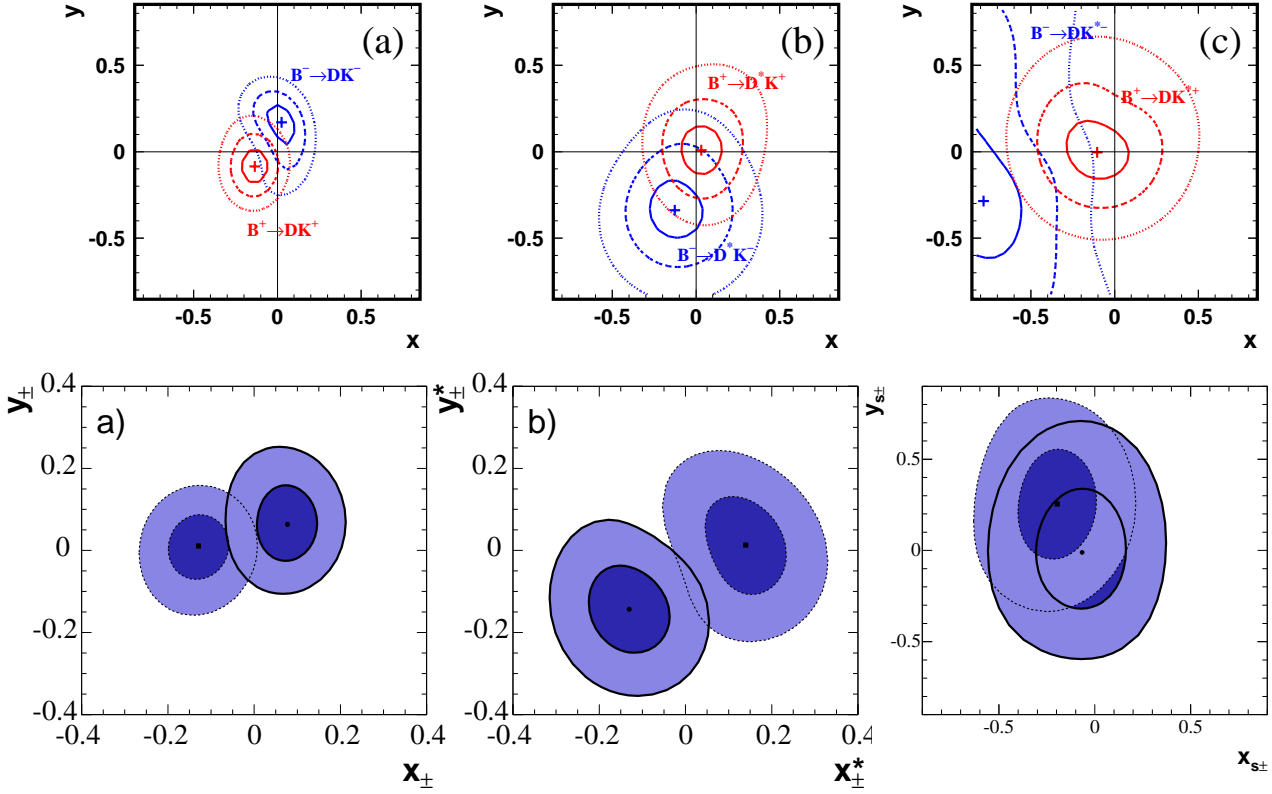


Figure 5: Results of signal fits in the (x, y) plane for (a) $B^+ \rightarrow DK^+$, (b) $B^+ \rightarrow D^*K^+$ and (c) $B^+ \rightarrow DK^{*+}$ samples, separately for B^- and B^+ data. Top: Belle 1, 2 and 3σ confidence contours. Blue is B^- , red is B^+ . Bottom: BABAR 1σ (dark) and 2σ (light) confidence contours. Solid is B^- , dashed is B^+ .

Table III Summary of BaBar and Belle measurements of the Dalitz analysis (GGSZ) observables x_{\pm} and y_{\pm} .

Mode	Experiment	$N(B\bar{B})$	$x_- (10^{-2})$	$y_- (10^{-2})$	$x_+ (10^{-2})$	$y_+ (10^{-2})$
$B \rightarrow D^0 K$	BABAR[13]	227×10^6	$+8 \pm 7 \pm 3 \pm 2$	$+6 \pm 9 \pm 4 \pm 4$	$-13 \pm 7 \pm 3 \pm 3$	$+2 \pm 8 \pm 2 \pm 2$
	Belle [15]	386×10^6	$+3^{+7}_{-8} \pm 1$	$+17^{+9}_{-12} \pm 2$	$-14 \pm 7 \pm 2$	$-9 \pm 9 \pm 1$
	HFAG Avg. [8]	-	$+5 \pm 5 \pm 2$	$+11 \pm 7 \pm 2$	$-14 \pm 5 \pm 3$	$-3 \pm 6 \pm 2$
$B \rightarrow D^{*0} K$	BABAR[13]	227×10^6	$-13 \pm 9 \pm 3 \pm 2$	$-14 \pm 11 \pm 2 \pm 3$	$+14 \pm 9 \pm 3 \pm 3$	$+1 \pm 12 \pm 4 \pm 6$
	Belle [15]	386×10^6	$-13^{+17}_{-15} \pm 2$	$-34^{+17}_{-16} \pm 3$	$+3 \pm 12 \pm 1$	$+1 \pm 14 \pm 1$
	HFAG Avg. [8]	-	$-13 \pm 8 \pm 2$	$-20 \pm 9 \pm 3$	$+10 \pm 7 \pm 3$	$+1 \pm 9 \pm 6$
$B \rightarrow D^0 K^*$	BABAR[14]	227×10^6	$-20 \pm 20 \pm 11 \pm 3$	$+26 \pm 30 \pm 16 \pm 3$	$-7 \pm 23 \pm 13 \pm 3$	$-1 \pm 32 \pm 18 \pm 5$
	Belle [15]	386×10^6	$-78^{+25}_{-30} \pm 3$	$-28^{+44}_{-34} \pm 5$	$-11^{+18}_{-17} \pm 1$	$0 \pm 16 \pm 1$
	HFAG Avg. [8]	-	$-46 \pm 17 \pm 3$	$+5 \pm 27 \pm 3$	$-10 \pm 15 \pm 3$	$0 \pm 15 \pm 5$

known. Both BABAR and Belle extract $A_D(m_{\pm}^2, m_{\pm}^2)$ by fitting high purity tagged $D^{*+} \rightarrow D^0 \pi^+$, $D^0 \rightarrow K_s^0 \pi^+ \pi^-$ samples using an Isobar Model [Coherent sum of 16 (15) Breit-Wigner amplitudes for BABAR (Belle), plus a non-resonant component] to model the D^0 decay amplitude. The Dalitz regions corresponding to the Doubly-Cabibbo suppressed decays $D^0 \rightarrow K^{*+} (892) \pi^-$ and $D^0 \rightarrow K^{*+} (1430) \pi^-$ [“ADS like”] and to the CP-odd decays $D^0 \rightarrow K_s^0 \rho^0$ decays [“GLW” like] are found to have the largest sensitivity to γ . Both BABAR and Belle introduce the cartesian coordinates $x_{\pm} = \text{Re}(r_B e^{i(\delta_B \pm \gamma)})$ and $y_{\pm} = \text{Im}(r_B e^{i(\delta_B \pm \gamma)})$

to fit their data. A total of 12 parameters (3×4) is extracted by each experiment from the Dalitz plot density fit of the D^0 in $B^{\pm} \rightarrow D^0 K^{\pm}$, $B^{\pm} \rightarrow D^{*0} K^{\pm}$ and $B^{\pm} \rightarrow D^0 K^{*\pm}$ data.

Using a sample of $227 \times 10^6 B\bar{B}$ events, BABAR reconstructs 282 ± 20 events in the $B \rightarrow D^0 K$ channel, 90 ± 11 (44 ± 8) in the $B \rightarrow D^{*0} K$, $D^{*0} \rightarrow D^0 \pi^0$ ($D^{*0} \rightarrow D^0 \gamma$) channel and 42 ± 8 events in the $B \rightarrow D^0 K^*$ channel. Belle reconstructs $331 \pm 17 D^0 K$, $81 \pm 8 D_{[D^0 \pi^0]}^{*0} K$ and $54 \pm 8 D^0 K^*$ events out of 357 fb^{-1} of data ($\sim 386 \times 10^6 B\bar{B}$ events). The results of the fits of the (x_{\pm}, y_{\pm}) parameters from

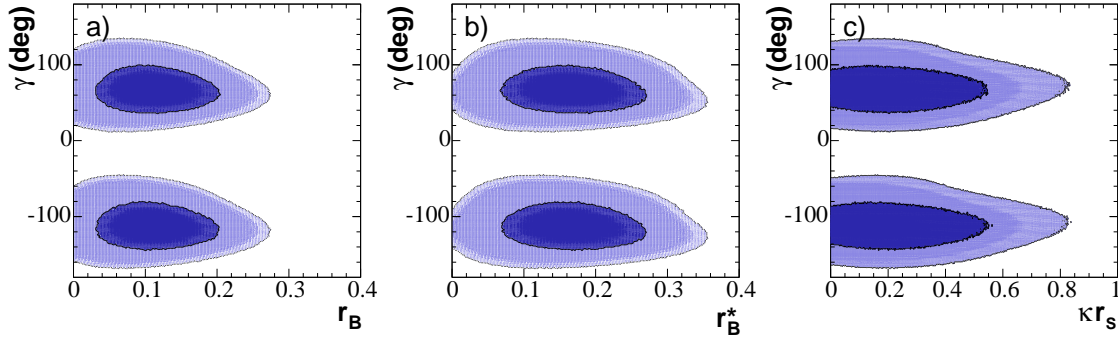


Figure 6: *BABAR* analysis: two-dimensional projections onto the (a) $r_B - \gamma$, (b) $r_B^* - \gamma$, and (c) $\kappa r_s - \gamma$ planes of the seven-dimensional one- (dark) and two- (light) standard deviation regions, for the combination of $B^- \rightarrow \tilde{D}^{(*)0} K^-$ and $B^- \rightarrow \tilde{D}^0 K^{*-}$ modes.

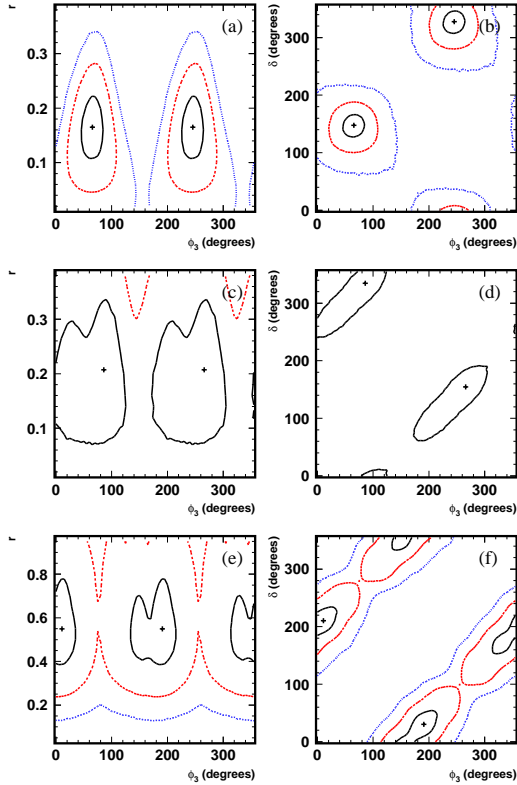


Figure 7: *Belle* analysis: two-dimensional projections onto the $(r_B - \gamma/\phi_3)$ plane (left) and the $(\delta_B - \gamma/\phi_3)$ plane (right) for the (a,b) $B^- \rightarrow D^0 K^-$, (c,d) $B^- \rightarrow D^{*0} K^-$, and (e,f) $B^- \rightarrow D^0 K^{*-}$ modes. Contours indicate 1, 2 and 3 σ confidence regions.

BABAR and *Belle* for the different B decay channels are shown in Fig.5 and summarized in Table III. A significant separation between the B^+ and the B^- data, indicative of direct CP violation, is visible in the $D^0 K$ and $D^{*0} K$ data. Both experiments use a frequentist analysis to interpret the constraints on $(x_{\pm}$,

$y_{\pm})$ in terms of the physical parameters $(r_B, \delta_B$ and $\gamma)$. From the combination of the different B decay channels, the two-dimensional constraints obtained by *BABAR* in the (r_B, γ) plane for DK , D^*K and DK^* are shown in Fig.6. The value of γ is constrained by *BABAR* to be $67^\circ \pm 28^\circ \pm 13^\circ \pm 11^\circ$, where the first error is statistical, the second one is the experimental systematic uncertainty and third reflects the Dalitz model uncertainty. The values found by *BABAR* for r_B are $r_B = 0.12 \pm 0.08 \pm 0.03 \pm 0.04$ for the $B^- \rightarrow DK^-$ mode, $r_B = 0.17 \pm 0.10 \pm 0.03 \pm 0.03$ for the $B^- \rightarrow D^*K^-$ mode and $r_B < 0.50(0.75)$ at one (two) standard deviation level for the $B^- \rightarrow DK^{*-}$ mode. The equivalent constraints from *Belle* on the (r_B, γ) and (δ_B, γ) planes are shown in Fig.7. *Belle* reports $\gamma/\phi_3 = 53^\circ \pm 15^\circ \pm 3^\circ \pm 9^\circ$ and finds for the ratio r_B of the two interfering amplitudes $r_B = 0.159^{+0.054}_{-0.050} \pm 0.012 \pm 0.049$ for the $B^- \rightarrow DK^-$ mode, $r_B = 0.175^{+0.108}_{-0.099} \pm 0.013 \pm 0.049$ for the $B^- \rightarrow D^*K^-$ mode and $r_B = 0.564^{+0.216}_{-0.155} \pm 0.041 \pm 0.084$ for the $B^- \rightarrow DK^{*-}$ mode. More details on the analysis are given in Ref.[13, 14, 15].

3. $\sin(2\beta + \gamma)$ measurements

Time-dependent asymmetries in $B^0 \rightarrow D^{(*)}\pi$, $D^{(*)}\rho$ and $B^0 \rightarrow D^{(*)0}K^0$ can be used to constrain $\sin(2\beta + \gamma)$ [16]. As β is well known from $b \rightarrow c\bar{c}s$, a constraint on the angle γ follows. The $B^0 \rightarrow D^{(*)}\pi$ method uses an interference between the usual Cabibbo-favored $b \rightarrow c$ channel and the doubly-Cabibbo suppressed $b \rightarrow u$ channel (Fig.8). These two amplitudes have a relative weak phase of γ , and a weak phase of 2β is provided by the $B^0\bar{B}^0$ mixing. These modes have the advantage of a "large" ($\sim 0.5\%$) branching fraction but the price to pay is the small ra-

ratio r of the suppressed to favored amplitudes,

$$r = \left| \frac{A(B^0 \rightarrow D^{(*)+}h^-)}{A(\bar{B}^0 \rightarrow D^{(*)+}h^-)} \right| \propto \lambda^2 (\sim 0.02).$$

This results in very small CP-asymmetries. Moreover, the ratio r cannot be measured directly, but has to be estimated from the measurement of $\mathcal{B}(B^0 \rightarrow D_s^+ \pi^-)$, assuming SU(3) flavor symmetry.

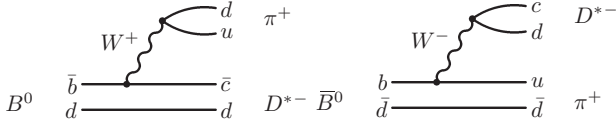


Figure 8: Feynman diagrams for the Cabibbo-favored decay $B^0 \rightarrow D^{*-} \pi^+$ (left) and the Cabibbo-suppressed decay $\bar{B}^0 \rightarrow D^{*-} \pi^+$ (right). The CKM-suppression factor is $|V_{cd}V_{ub}^*/V_{cb}V_{ud}^*| \propto \lambda^2 \sqrt{\rho^2 + \eta^2} \approx 0.02$.

The experimental observables are the coefficients S^\pm and C of the $\sin(\Delta m \Delta t)$ and $\cos(\Delta m \Delta t)$ terms in the time dependent asymmetries of $B^0(\bar{B}^0) \rightarrow D^{(*)\pm} \pi^\mp$ (or $D^{(*)\pm} \rho^\mp$). For small values of r , the parameter S^\pm is given by $S^\pm \simeq 2r \sin(2\beta + \gamma \pm \delta)$, where δ is the strong phase difference between the $b \rightarrow u$ and $b \rightarrow c$ decay amplitudes.

Potential competing CP violating effects can arise from $b \rightarrow u$ transitions on the tag side if a Kaon is used to tag the flavor of the other B^0 in the event, resulting in an additional \sin term $S'^\pm = 2r' \sin(2\beta + \gamma \pm \delta')$. Here, r' (δ') are the effective amplitude (phase) used to parameterize the tag side interference. To account for this term, BABAR chooses to rewrite S^\pm as $S^\pm = (a \pm c) + b$, where $a = 2r \sin(2\beta + \gamma) \cos(\delta)$, $c = \cos(2\beta + \gamma)[2r \sin(\delta) + 2r' \sin(\delta')]$ and $b = 2r' \sin(2\beta + \gamma) \cos(\delta')$. This parametrization has the advantage that the a parameter does not depend on the tagging category. On the other hand, the c parameter can only be estimated with lepton-tagged events, for which one has $c = c^{\text{lept}} = \cos(2\beta + \gamma)[2r \sin(\delta)]$. The b parameter characterizes CP violation on the tag side and does not contribute to the interpretation. In the approach chosen by BABAR, the a and c^{lept} parameters are fitted. Belle, on the contrary, chooses to fit the S^\pm parameters but measures tag-side CPV parameters S'^\pm using a sample of $D^* \nu \bar{\nu}$ events, which can have only tag-side CP-violation.

BABAR and Belle use two experimental methods for reconstructing $B^0(\bar{B}^0) \rightarrow D^{(*)} \pi$ and $D^{(*)} \rho$ decays. They perform either exclusive reconstruction, where the hadronic decay modes with $D^0 \rightarrow K^- \pi^+$, $K^- \pi^+ \pi^0$ and $K^- \pi^+ \pi^- \pi^+$ are fully reconstructed, or partial reconstruction of $D^{*\pm} \pi^\mp$, where only the slow π , and not the D^0 from $D^* \rightarrow D^0 \pi$, is reconstructed. Using only the slow pion provides sufficient kinematic constraints to reconstruct this decay. The fully exclusive method has a very high signal purity [typically

larger than 90%] but a lower efficiency. The semi-inclusive method has efficiencies 5 times larger but the purity is only $\sim 30\%$ [$\sim 50\%$] for Kaon [Lepton] tags.

BABAR has published results based on a statistics of 232×10^6 $B\bar{B}$ events [17]. From 18710 $D^{*\pm} \pi^\mp$ events tagged with a lepton (purity 54%), and 70580 $D^{*\pm} \pi^\mp$ events tagged with a kaon (purity 31%) the parameters related to $2\beta + \gamma$ are measured to be

$$\begin{aligned} a_{D^* \pi} &= 2r \sin(2\beta + \gamma) \cos \delta \\ &= -0.034 \pm 0.014 \pm 0.009 \end{aligned}$$

and

$$\begin{aligned} c_{D^* \pi}^{\text{lept}} &= 2r \cos(2\beta + \gamma) \sin \delta \\ &= -0.019 \pm 0.022 \pm 0.013, \end{aligned}$$

where the first error is statistical and the second is systematic. This is the world most precise measurement of CP-violating parameters in $B \rightarrow D^{(*)} \pi$ decays to date. BABAR has also published results based on a statistics of 232×10^6 $B\bar{B}$ events for the fully exclusive analysis of $B^0 \rightarrow D \pi$, $D^* \pi$ and $D \rho$ [18]. From a time-dependent maximum likelihood fit to a sample of 15038 $D^\pm \pi^\mp$ events (purity 87%), 14002 $D^{*\pm} \pi^\mp$ events (purity 87%), and 8736 $D^\pm \rho^\mp$ events (purity 82%), the parameters related to the CP violation angle $2\beta + \gamma$ are measured to be:

$$\begin{aligned} a_{D \pi} &= -0.010 \pm 0.023 \pm 0.007, \\ c_{D \pi}^{\text{lept}} &= -0.033 \pm 0.042 \pm 0.012, \\ a_{D^* \pi} &= -0.040 \pm 0.023 \pm 0.010, \\ c_{D^* \pi}^{\text{lept}} &= +0.049 \pm 0.042 \pm 0.015, \\ a_{D \rho} &= -0.024 \pm 0.031 \pm 0.009, \\ c_{D \rho}^{\text{lept}} &= -0.098 \pm 0.055 \pm 0.018, \end{aligned}$$

where the first error is statistical and the second is systematic. These results are combined with the result obtained on the partially reconstructed

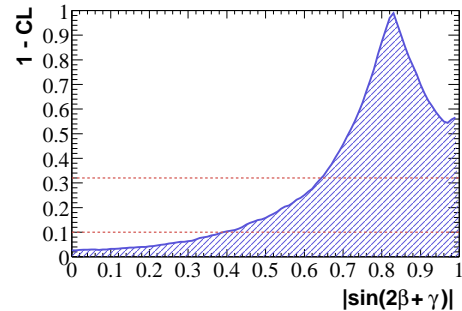


Figure 9: Frequentist confidence level as a function of $|\sin(2\beta + \gamma)|$, obtained when combining the BABAR results on exclusive decays with the result obtained on partially reconstructed $B \rightarrow D^{*\pm} \pi^\mp$ decays [17]. The horizontal lines show the 68% (top) and 90% C.L. (bottom).

$B \rightarrow D^{*\pm} \pi^\mp$ sample, using a frequentist method described in Ref. [17] to set a constraint on $2\beta + \gamma$. Based on the results from Refs.[19, 20], the values of the amplitude ratios $r_{D^*\pi}$, $r_{D\pi}$ and $r_{D\rho}$ used to set this constraint are:

$$\begin{aligned} r_{D^*\pi} &= 0.015^{+0.004}_{-0.006} \pm 0.005(\text{theory}), \\ r_{D\pi} &= 0.019 \pm 0.004 \pm 0.006(\text{theory}), \\ r_{D\rho} &= 0.003 \pm 0.006 \pm 0.001(\text{theory}) \end{aligned}$$

The confidence level as a function of $|\sin(2\beta + \gamma)|$ is shown in Fig. 9 and *BABAR* sets the lower limits $|\sin(2\beta + \gamma)| > 0.64$ (0.40) at 68% (90%) C.L.

For the 2006 winter conferences, Belle has released a new result based on an integrated luminosity of 357 fb^{-1} , corresponding to approximately 386×10^6 $B\bar{B}$ events [21]. The CP violation parameters used in the Belle analysis are

$$S^\pm = \frac{2(-1)^L r \sin(2\phi_1 + \phi_3 \pm \delta)}{(1 + r^2)}, \quad (6)$$

where L is the orbital angular momentum of the final state (1 for $D^*\pi$ and 0 for $D\pi$), and δ is the strong phase difference of the V_{cb} and V_{ub} amplitudes. The values of r and δ depend on the choice of the final states, and are denoted with subscripts $D^*\pi$ and $D\pi$ in what follows. It should be noted that the definition of the S^\pm parameter used by *BABAR* and Belle differ by a factor $(-1)^L$. With the partial reconstruction method, 21741 $D^*\pi$ events tagged by a lepton from the opposite B decay are reconstructed, and the purity is 66%. With the fully exclusive reconstruction, 31491 $D^*\pi$ events (purity 89%) and 31725 $D\pi$ events (purity 83%) are reconstructed (all tags). The final results expressed in terms of S^+ and S^- , which are related to the CKM angles β/ϕ_1 and γ/ϕ_3 , the ratio of suppressed to favoured amplitudes, and the strong phase difference between them, as $S^\pm = -r_{D^*\pi} \sin(2\beta + \gamma \pm \delta_{D^*\pi}) / (1 + r_{D^*\pi}^2)$ for $D^*\pi$ and $S^\pm = +r_{D\pi} \sin(2\phi_1 + \phi_3 \pm \delta_{D\pi}) / (1 + r_{D\pi}^2)$ for $D\pi$, are

$$\begin{aligned} S^+(D^*\pi) &= 0.049 \pm 0.020 \pm 0.011, \\ S^-(D^*\pi) &= 0.031 \pm 0.019 \pm 0.011, \\ S^+(D\pi) &= 0.031 \pm 0.030 \pm 0.012, \\ S^-(D\pi) &= 0.068 \pm 0.029 \pm 0.012, \end{aligned}$$

where the first errors are statistical and the second errors are systematic. These results are shown in Fig. 10 in terms of 1σ , 2σ and 3σ allowed regions in the S^- versus S^+ space. They are an indication of CP violation in $B^0 \rightarrow D^{*-}\pi^+$ and $B^0 \rightarrow D^-\pi^+$ decays at the 2.5σ and 2.2σ levels, respectively.

Using published *BABAR* and Belle measurements of $\mathcal{B}(B^0 \rightarrow D_s^{(*)+} \pi^-)$ plus some theoretical assumptions based on SU(3) symmetry, the Belle collaboration estimates the values of the amplitude ratios $r_{D^*\pi}$ and

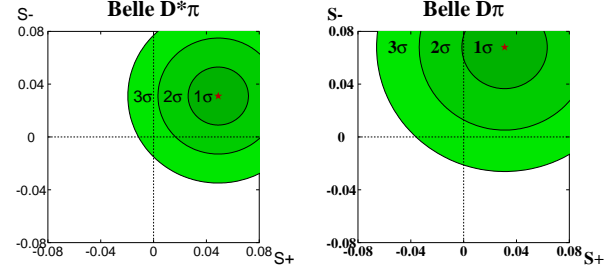


Figure 10: Results of the S^\pm measurements expressed in terms of S^- vs S^+ for the $D^*\pi$ (left) and $D\pi$ (right) modes. Shaded regions indicate allowed regions with 1σ , 2σ and 3σ uncertainties defined by $\sqrt{-2\ln\mathcal{L}} = 1, 4, 9$, respectively

$r_{D\pi}$ to be

$$\begin{aligned} r_{D^*\pi} &= 0.020 \pm 0.007 \pm 0.006(\text{theory}), \\ r_{D\pi} &= 0.021 \pm 0.004 \pm 0.006(\text{theory}) \end{aligned}$$

Using these values, they obtain 68% (95%) confidence level lower limits on $|\sin(2\beta + \gamma)|$ of 0.44 (0.13) and 0.52 (0.07) from the $D^*\pi$ and $D\pi$ modes, respectively.

In order to compare and average the *BABAR* and Belle results, the HFAG group [8] has converted the Belle results to express them in terms of the parameters a and c used in the *BABAR* experiment. A comparison of these results, together with the corresponding averages, is shown in Fig.11. Individual measurements of a with a statistical significance better than 3σ should be within reach before the end of the B-factory era.

4. $\mathcal{B}(B^0 \rightarrow D_s^{(*)+} \pi^-)$

BABAR has recently submitted for publication a new measurement of the $B^0 \rightarrow D_s^{(*)+} \pi^-$ and $B^0 \rightarrow D_s^{(*)+} K^-$ branching fractions, based on a data sample of 230×10^6 $B\bar{B}$ events [23]. As explained in the previous section, the decay $B^0 \rightarrow D_s^{(*)+} \pi^-$ is interesting because it can be used to estimate the suppressed to favored amplitude ratios $r_{D^{(*)}\pi}$ in the $2\beta + \gamma$ analysis of the $B^0 \rightarrow D^{(*)+} \pi^-$ channel [16]:

$$r_{D^{(*)}\pi} = \tan \theta_c \frac{f_{D^{(*)}}}{f_{D_s^{(*)}}} \sqrt{\frac{\mathcal{B}(B^0 \rightarrow D_s^{(*)+} \pi^-)}{\mathcal{B}(B^0 \rightarrow D^{(*)+} \pi^-)}}, \quad (7)$$

where θ_c is the Cabibbo angle, and $f_{D^{(*)}}/f_{D_s^{(*)}}$ is the ratio of $D^{(*)}$ and $D_s^{(*)}$ meson decay constants [22]. Other SU(3)-breaking effects are believed to affect $r_{D^{(*)}\pi}$ by less than 30%.

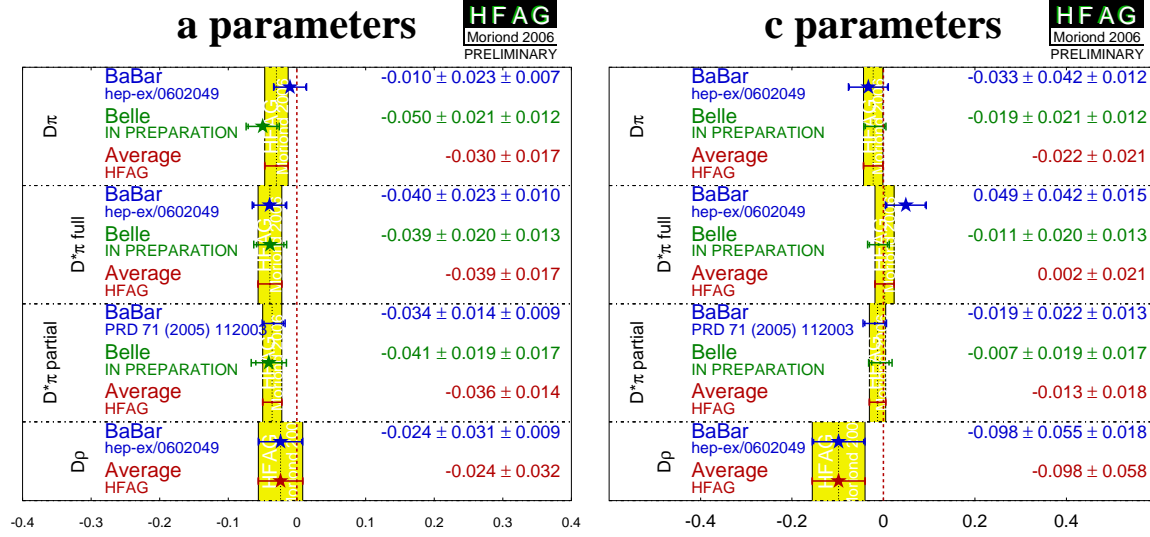


Figure 11: Comparison of *BABAR* and *Belle* $\sin(2\beta + \gamma)$ results and HFAG averages for the different channels [8].

From the number of signal events observed, *BABAR* computes the following branching fractions:

$$\begin{aligned}\mathcal{B}(B^0 \rightarrow D_s^+ \pi^-) &= (1.3 \pm 0.3 \pm 0.2) \times 10^{-5} \\ \mathcal{B}(B^0 \rightarrow D_s^{*+} \pi^-) &= (2.8 \pm 0.6 \pm 0.5) \times 10^{-5} \\ \mathcal{B}(B^0 \rightarrow D_s^+ K^-) &= (2.5 \pm 0.4 \pm 0.4) \times 10^{-5} \\ \mathcal{B}(B^0 \rightarrow D_s^{*+} K^-) &= (2.0 \pm 0.5 \pm 0.4) \times 10^{-5}\end{aligned}$$

Assuming $SU(3)$ relation, Eq. (7), the following values of the amplitude ratio r are determined:

$$\begin{aligned}r_{D\pi} &= (1.3 \pm 0.2(\text{stat}) \pm 0.1(\text{syst})) \times 10^{-2} \\ r_{D^* \pi} &= (1.9 \pm 0.2(\text{stat}) \pm 0.2(\text{syst})) \times 10^{-2}.\end{aligned}$$

This implies small CP asymmetries in $B^0 \rightarrow D^{(*)} \mp \pi^\pm$ decays.

5. Search for $B^0 \rightarrow D_s^{(*)+} a_{0(2)}^-$

It was recently suggested to use the decays $B^0 \rightarrow D^{(*)+} a_{0(2)}^-$ for measuring $\sin(2\beta + \gamma)$ [24]. These decay can proceed through the two diagrams shown in Fig.12 and it is expected that the V_{cb} amplitude is significantly suppressed respective to the V_{ub} amplitude, giving significant CP -asymmetries.

The V_{ub} -mediated part of the $B^0 \rightarrow D^{(*)+} a_{0(2)}^-$ decay amplitude can be related to $B^0 \rightarrow D_s^{(*)+} a_{0(2)}^-$ using $\tan(\theta_{\text{Cabibbo}}) = |V_{cd}/V_{cs}|$ and the ratio of the decay constants $f_{D^{(*)}}/f_{D_s^{(*)}}$. Branching fractions of $B^0 \rightarrow D_s^{(*)+} a_2^-$ are predicted to be in the range 1.3–1.8 (2.1–2.9) in units of 10^{-5} [26]. Branching fraction estimates for $B^0 \rightarrow D_s^{(*)+} a_0^-$ of approximately

8×10^{-5} are obtained using $SU(3)$ symmetry from the predictions made for $B^0 \rightarrow D^{(*)+} a_0^-$ in [25].

BABAR finds no evidence for these decays and set upper limits at 90% C.L. on the branching fractions [27]: $\mathcal{B}(B^0 \rightarrow D_s^+ a_0^-) < 1.9 \times 10^{-5}$, $\mathcal{B}(B^0 \rightarrow D_s^{*+} a_0^-) < 3.6 \times 10^{-5}$, $\mathcal{B}(B^0 \rightarrow D_s^+ a_2^-) < 1.9 \times 10^{-4}$, and $\mathcal{B}(B^0 \rightarrow D_s^{*+} a_2^-) < 2.0 \times 10^{-4}$. These upper limits suggest that the branching ratios of $B^0 \rightarrow D^{(*)+} a_{0(2)}^-$ are too small for CP -asymmetry measurements given the present statistics of the B -factories.

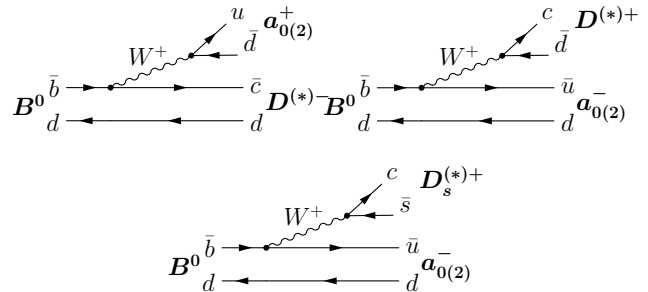


Figure 12: Top diagrams: tree diagrams contributing to the decay amplitude of $B^0 \rightarrow D^{(*)-} a_{0(2)}^+$ (including the $B^0 \bar{B}^0$ mixing mediated part of the amplitude). Bottom diagram: tree diagram representing the decay amplitude of $B^0 \rightarrow D_s^{(*)+} a_{0(2)}^-$.

6. Study of $B^0 \rightarrow D^{(*)0} K^{(*)0}$

The decay modes $\bar{B}^0 \rightarrow D^{(*)0} \bar{K}^0$ offer a new approach for the determination of $\sin(2\beta + \gamma)$ from the measurement of time-dependent CP asymmetries in these decays. The CP asymmetry appears as a result of the interference between two diagrams leading to the same final state $D^{(*)0} K_s^0$ (Figure 13). A \bar{B}^0 meson can either decay via a $b \rightarrow c$ quark transition to the $D^{(*)0} \bar{K}^0$ ($\bar{K}^0 \rightarrow K_s^0$) final state, or oscillate into a B^0 which then decays via a $\bar{b} \rightarrow \bar{u}$ transition to the $D^{(*)0} K^0$ ($K^0 \rightarrow K_s^0$) final state. The $\bar{B}^0 B^0$ oscillation provides the weak phase 2β and the relative weak phase between the two decay diagrams is γ .

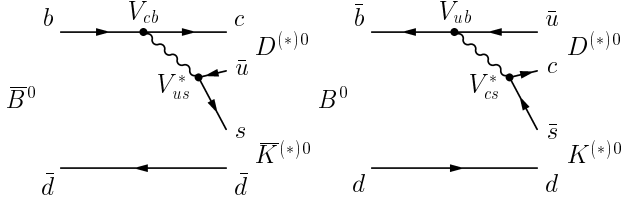


Figure 13: The decay diagrams for the $b \rightarrow c$ transition $\bar{B}^0 \rightarrow D^{(*)0} \bar{K}^0$ and the $\bar{b} \rightarrow \bar{u}$ transition $B^0 \rightarrow D^{(*)0} K^0$.

The sensitivity of this method depends on the rates for these decays and the ratio $r_B^{(*)}$ of the decay amplitudes, $r_B^{(*)} \equiv |\mathcal{A}(\bar{B}^0 \rightarrow \bar{D}^{(*)0} \bar{K}^0)|/|\mathcal{A}(\bar{B}^0 \rightarrow D^{(*)0} \bar{K}^0)|$. In the Standard Model $r_B^{(*)} = f \cdot |V_{ub} V_{cs}^*|/|V_{cb} V_{us}^*| \approx f \cdot 0.4$, where the factor f accounts for the difference in the strong interaction dynamics between the $b \rightarrow c$ and $b \rightarrow u$ processes. There are no theoretical calculations or experimental constraints on f . A direct determination of $r_B^{(*)}$ from the measured rates for $\bar{B}^0 \rightarrow D^{(*)0} \bar{K}^0$ ($\bar{K}^0 \rightarrow K_s^0$) decays is not possible, because one cannot distinguish between $\bar{B}^0 \rightarrow D^{(*)0} \bar{K}^0$ and $B^0 \rightarrow D^{(*)0} K^0$. However, insight into the B decay dynamics affecting $r_B^{(*)}$ can be gained by measuring a similar amplitude ratio $\tilde{r}_B \equiv |\mathcal{A}(\bar{B}^0 \rightarrow \bar{D}^0 \bar{K}^{*0})|/|\mathcal{A}(\bar{B}^0 \rightarrow D^0 \bar{K}^{*0})|$ using the self-tagging decay $\bar{K}^{*0} \rightarrow K^- \pi^+$.

BABAR has recently submitted for publication a new measurement of the $B^0 \rightarrow D^{(*)0} K_s^0$, $\bar{B}^0 \rightarrow D^0 \bar{K}^{*0}$ and $\bar{B}^0 \rightarrow \bar{D}^0 \bar{K}^{*0}$ branching fractions, based on a data sample of 226×10^6 $B\bar{B}$ events [28]. Defining $\mathcal{B}(\bar{B}^0 \rightarrow D^{*0} \bar{K}^0) \equiv (\mathcal{B}(\bar{B}^0 \rightarrow D^{*0} \bar{K}^0) + \mathcal{B}(B^0 \rightarrow D^{*0} K^0))/2$ and $\mathcal{B}(\tilde{B}^0 \rightarrow D^0 \bar{K}^0) \equiv (\mathcal{B}(\bar{B}^0 \rightarrow D^0 \bar{K}^0) + \mathcal{B}(B^0 \rightarrow D^0 K^0))/2$, the results of this measurement are:

$$\begin{aligned} \mathcal{B}(\tilde{B}^0 \rightarrow D^0 \bar{K}^0) &= (5.3 \pm 0.7 \pm 0.3) \times 10^{-5} \\ \mathcal{B}(\tilde{B}^0 \rightarrow D^{*0} \bar{K}^0) &= (3.6 \pm 1.2 \pm 0.3) \times 10^{-5} \\ \mathcal{B}(\bar{B}^0 \rightarrow D^0 \bar{K}^{*0}) &= (4.0 \pm 0.7 \pm 0.3) \times 10^{-5} \\ \mathcal{B}(\bar{B}^0 \rightarrow \bar{D}^0 \bar{K}^{*0}) &< 1.1 \times 10^{-5} \text{ at 90\% C.L.} \end{aligned}$$

This measurement is in good agreement with previous results from Belle [29]. From the absence of signal for the V_{ub} mediated mode $\bar{B}^0 \rightarrow \bar{D}^0 \bar{K}^{*0}$, the limit $\tilde{r}_B < 0.40$ at 90% C.L. is obtained. The present signal yields combined with this limit on \tilde{r}_B suggest that a substantially larger data sample is needed for a competitive time-dependent measurement of $\sin(2\beta + \gamma)$ in $\bar{B}^0 \rightarrow D^{(*)0} \bar{K}^0$ decays.

7. Conclusion

Although the angle γ/ϕ_3 is the most difficult to measure of the Unitarity Triangle angles at the B-factories, very promising progress has been made in constraining it over the past few years. With the increase of statistics expected between now and 2008, and because these measurements are theoretically clean, both γ and $\sin(2\beta + \gamma)$ will progress toward becoming precision measurements before the end of the decade.

Acknowledgments

As a member of the BABAR collaboration, I would like to thank my BABAR and PEP-II colleagues for their support and for choosing me to present these results. I want also to thank Karim Trabelsi for useful discussions about the Belle results. Finally, I wish to thank the organizers for a successful and very enjoyable conference.

References

- [1] M. Gronau and D. London, Phys. Lett. B **253**, 483 (1991); M. Gronau and D. Wyler, Phys. Lett. B **265**, 172 (1991);
- [2] D. Atwood, I. Dunietz and A. Soni, Phys. Rev. Lett. **78**, 3257 (1997).
- [3] A. Giri, Yu. Grossman, A. Soffer and J. Zupan, Phys. Rev. D **68**, 054018 (2003).
- [4] BABAR Collaboration, B. Aubert et al., Phys. Rev. **D73**, 051105(R)(2006).
- [5] Belle Collaboration, K. Abe et al., Phys. Rev. **D73**, 051106(R)(2006).
- [6] BABAR Collaboration, B. Aubert et al., Phys. Rev. **D71**, 031102 (2005).
- [7] BABAR Collaboration, B. Aubert et al., Phys. Rev. **D72**, 071103 (2005).
- [8] <http://www.slac.stanford.edu/xorg/hfag/triangle/moriond2006/index.shtml>.
- [9] BABAR Collaboration, B. Aubert et al., Phys. Rev. Lett. **91**, 171801 (2003).

- [10] *BABAR* Collaboration, B. Aubert et al., Phys. Rev. **D72** 032004 (2005).
- [11] *BABAR* Collaboration, B. Aubert et al., Phys. Rev. **D72** 071104 (2005).
- [12] Belle Collaboration, K. Abe et al., hep-ex/0508048, Contributed to EPS International Europhysics Conference on High Energy Physics (HEPP-EPS 2005), Lisbon
- [13] *BABAR* Collaboration, B. Aubert et al., Phys. Rev. Lett. **95**, 121802 (2005).
- [14] *BABAR* Collaboration, B. Aubert et al., hep-ex/0507101
- [15] Belle Collaboration, K. Abe et al., hep-ex/0604054, submitted to PRD.
- [16] I. Dunietz, Phys. Lett. **B427**, 179 (1998).
- [17] *BABAR* Collaboration, B. Aubert et al., Phys. Rev. **D71** 112003 (2005).
- [18] *BABAR* Collaboration, B. Aubert et al., hep-ex/0602049, submitted to PRD-RC.
- [19] *BABAR* Collaboration, B. Aubert et al., Phys. Rev. Lett. **90**, 181803 (2003).
- [20] *BABAR* Collaboration, B. Aubert et al., hep-ex/0408029, submitted to ICHEP2004.
- [21] Belle Collaboration, F.J. Ronga et al., hep-ex/0604013, submitted to Phys. Rev. **D**.
- [22] C. Aubin et al., Phys. Rev. Lett. **95** 122002 (2005); D. Becirevic, preprint hep-ph/0310072 (2003).
- [23] *BABAR* Collaboration, B. Aubert et al., hep-ex/0604012, submitted to Phys. Rev. Lett..
- [24] M. Diehl, G. Hiller, Phys. Lett. **B 517**, 125 (2001).
- [25] M. Diehl, G. Hiller, JHEP 0106:067 (2001).
- [26] C.S. Kim, J.P. Lee, and S. Oh, Phys. Rev. **D 67**, 014011 (2003).
- [27] *BABAR* Collaboration, B. Aubert et al., Phys. Rev. **D73** (2006) 071103.
- [28] *BABAR* Collaboration, B. Aubert et al., hep-ex/0604016, submitted to PRD-RC.
- [29] Belle Collaboration, P. Krokovny et al., Phys. Rev. Lett. **90**, 141802 (2003).